

VISCOELASTIC CHARACTERIZATION OF THIN-FILM
POLYMERS EXPOSED TO LOW EARTH ORBIT

Alan Letton

*Polymer Technology Center
Mechanical Engineering Department
Texas A & M University
College Station, Texas 77843*

*Allan Farrow, Thomas Strganac
Aerospace Engineering Department
Texas A & M University
College Station, Texas 77843*

ABSTRACT

The materials made available through the LDEF satellite provide a set of specimens that can be well characterized and have a known exposure history with reference to atomic oxygen and ultraviolet radiation exposure. Mechanical characteristics measured from control samples and exposed samples provide a data base for predicting the behavior of polymers in low earth orbit.

Samples of 1.0 mil thick low density polyethylene were exposed to the low earth orbit environment for a period of six years. These materials were not directly exposed to ram atomic oxygen and offer a unique opportunity for measuring the effect of atomic oxygen and UV radiation on mechanical properties with little concern to the effect of erosion. The viscoelastic characteristics of these materials were measured and compared to the viscoelastic characteristics of control samples. To aid in differentiating the effects of changes in crystallinity resulting from thermal cycling, from the effects of changes in chemical structure resulting from atomic oxygen/UV attack to the polymer, a second set of control specimens, annealed to increase crystallinity, were measured as well. The resulting characterization of these materials will offer insight into the impact of atomic oxygen/UV on the mechanical properties of polymeric materials.

The viscoelastic properties measured for the control, annealed, and exposed specimens were the storage and loss modulus as a function of frequency and temperature. From these datum is calculated the viscoelastic master curve derived using the principle of time/temperature superposition.¹ Using this master curve, the relaxation modulus is calculated using the method of Ninomiya and Ferry.¹ The viscoelastic master curve and the stress relaxation modulus provide a direct measure of the changes in the chemical or morphological structure. In addition, the effect of these changes on long-term and short-term mechanical properties is known directly. It should be noted that the dependence on directionality for the polymer films has been considered since these films were manufactured by a blown-film process.²

INTRODUCTION

It is known that thin film polymers unprotected from direct ram impact of atomic oxygen in the low earth orbit (LEO) environment undergo significant degradation. This degradation is synergistically increased in the presence of high levels of ultra-violet (UV) radiation³. To date, the large body of knowledge associated with the use of polymers in LEO has probed the chemical mechanisms associated with atomic oxygen attack and UV exposure. The effect of atomic oxygen and UV radiation on engineering properties has been largely ignored. With the increasing importance of polymers' use in orbiting spacecraft it has become necessary to determine how and to what extent the mechanical properties of polymers are affected by the LEO environment.⁴

The polyolefin films studied here offer a unique opportunity since they were not directly exposed to the ram impact of atomic oxygen prevalent in most LEO studies. As a result of the configuration of the test tray aboard the Long Duration Exposure Facility (LDEF), the specimens studied here were exposed to diffuse atomic oxygen only (in the presence of UV radiation). This oxygen does not have the kinetic energy of 5eV typically associated with ram impact atomic oxygen. Materials studied were control, exposed and thermally annealed specimens of 1.0 mil Stratofilm[®]. Stratofilm[®] is a low density polyethylene (LDPE) film manufactured for use in scientific balloons.

OVERVIEW OF EXPOSED MATERIALS AND CONDITIONS

It has recently been observed that exposure of polymers to the LEO environment can result in significant weight loss, possibly due to degradation primarily from atomic oxygen attack.¹ Although it is recognized that the presence of atomic oxygen and UV radiation alters the chemical integrity of polymers, it is not known to what extent these chemical alterations affect the mechanical behavior of the material. Fortunately, the extended duration of the LDEF mission significantly enhanced the opportunities to characterize the morphological and mechanical properties of these exposed polymers. The findings of this research contribute to the predictive models of material constitutive characteristics. The balloon materials exposure experiment consists of 38 polymer film specimens and 24 fibrous cord specimens.^{3,4}

The mechanics of the orbit were such that one end of LDEF faced the Earth and one specific side was always aligned with the orbital velocity vector (or the "RAM" when referring to the direct exposure of atomic oxygen). The LDEF was inserted into a 476km orbit; when LDEF was retrieved, the orbit had decayed to 333 km.

The balloon materials exposure experiment consisted of 38 thin film polymer samples and 24 fibrous cord samples. The thin-film polymer samples ranged from 0.35 mil to 1.8 mil in thickness and were primarily constructed of polyester and polyethylene. Some of the thin-film specimens were reinforced with nylon, Kevlar, or polyester fibers. These polymeric materials are intended for use in long-duration scientific balloons and, except for the laminates and composite films, are manufactured as a blown film. This manufacturing process is known to introduce a biaxial orientation to the film resulting in anisotropic mechanical properties. Hence, pairs of specimens with mutually perpendicular orientation were included in the experiment package to account for directionality. Each non-reinforced specimen was six inches long and one inch wide. Each reinforced film was six inches long and one and one-half inches wide.

Spacecraft with the orbit of LDEF travel at a rate of 8 km/s. This velocity has the effect of providing the atomic oxygen in LEO with a translational energy of approximately 5 eV as it strikes surfaces perpendicular to the direction of RAM. Under these conditions many polymers are degraded with resulting mass loss. The balloon materials exposure experiment was positioned on row 6, which was oriented 90 degrees from the velocity vector (actually 98 degrees due to a slight misalignment). This yielded a significantly smaller AO fluence (2 orders of magnitude) than RAM facing experiments. Further, the specimens were shielded as the mounting trays were slightly recessed within the supporting LDEF structure.⁵

The fortuitous location of the balloon materials exposure experiment on LDEF minimized direct impact by atomic oxygen. Hence, the effect of the environment on balloon materials has been provided without the worry of atomic oxygen abrasion; as a result a majority of the materials survived the extended LDEF mission. The experiment was exposed to a minimum level of UV radiation by comparison to other locations aboard LDEF.⁶ Except for the earth-end experiment locations, the row containing these specimens was exposed to the lowest equivalent sun hours, 6500. By comparison, the space end of LDEF received the maximum exposure, which was 14,500 equivalent sun hours. Further, the slightly recessed position of the specimen trays provided shielding for the specimens.

EXPERIMENTAL PROCEDURE

A Rheometrics Solids Analyzer model II (RSA-II) was used for viscoelastic characterization. The RSA-II applies an oscillating tensile strain to a thin film specimen by clamping the specimen between two grips and driving one of the clamping fixtures at a designated frequency. The RSA-II is capable of testing specimens between the frequencies of 0.1 radians/second and 400 radians/second.

To measure the storage and loss moduli as a function of temperature the RSA II is equipped with an environmental chamber capable of attaining temperatures between -150°C and 450°C. Since the glass transition temperature of all the specimens tested is approximately -40°C, by testing the specimens to -150°C the entire glass transition region can be captured. Similarly, the melting temperature is approximately 100°C for the specimens tested. Therefore, the RSA-II allows the entire temperature range of interest, from the region previous to the glass transition to the melting temperature, to be captured.

Due to the design of the RSA-II there are inherent limitations on the size and compliance of the sample to be tested. The minimum specimen compliance that the RSA-II can measure is 40 $\mu\text{m}/\text{kg}$. Any sample with a compliance less than this will be subject to large measurement errors due to limits in the hardware transducer compliance correction. The maximum allowable compliance of a specimen is based on the sample being capable of generating a force equal to the lower limit of the transducer (1 gram force) with the maximum dynamic oscillation (± 0.5 mm). The combination of these two limiting factors leads to a maximum testable sample compliance of 5×10^5 $\mu\text{m}/\text{kg}$.

With the modulus of the sample fixed and the thickness of the sample determined by the film that was tested, the sample width was the only parameter available for adjustment in order to test within the RSA-II's recommended operating region. A thickness of approximately 0.02 mm and an estimated modulus of 2×10^{10} dynes/cm² for the test sample yielded an optimum sample width of between 6.0 mm and 4.5 mm.

In order to insure that the samples would only be tested in their linear range, such that time-temperature superposition is valid, a series of strain sweeps were conducted. This test was conducted at select temperatures and at select frequencies to insure linear measurements over the entire testing range. The nonlinear region of the strain sweep is characterized by a force decrease in the strain versus force curve. There is a simultaneous change in the values of the storage and loss moduli at the same value of strain where the force deviates from its linear behavior. When the storage and loss moduli are no longer independent of the strain, the beginning of the nonlinear region is noted. By performing the strain sweep at a number of temperatures, the linear/nonlinear boundary can be characterized as a function of strain and temperature. When characterizing the storage and loss moduli as functions of frequency and temperature, a strain that is less than the critical strain at which the nonlinear region begins at each temperature and frequency must be used in order to remain in the linear region. Also required is some level of pretension in the

specimen, used to keep the specimen from buckling during dynamic oscillations. The pretension force is chosen so that the dynamic force required to produce the largest strain at the highest frequency to be tested is less than the static pretension force. This will insure that the specimen will never buckle over the range of tested strains and frequencies. The frequency range that was tested was determined by the RSA-II's physical limitations. The maximum frequency of oscillation was 100 radians/second. The smallest frequency of oscillation used for testing was 0.4 radians/second.

Once the linear region of the material has been characterized, the RSA-II was again used to measure the viscoelastic response of the specimens as a function of frequency and temperature. An initial temperature of -150°C was chosen as a starting point for the viscoelastic characterization. The final temperature was determined by the material's melting point, approximately 100°C . The dynamic mechanical characterization of the specimen was continued until the specimen was unable to support the load needed for testing. This occurred at approximately 85°C .

The storage and loss moduli were recorded over a predetermined range of frequencies at discrete temperatures within a specified temperature range. A 5°C step size was chosen for these frequency-temperature sweeps, this step size allowed a significant amount of overlap in the frequency curves when the data was shifted. Although a smaller temperature step size would have allowed more data overlap, it would have also significantly increased the time necessary for the temperature to stabilize and increased the total time necessary to complete a test. To avoid problems associated with long term creep resulting from the static pretension the temperature frequency sweeps were conducted in three sections. The first section of testing covered the temperature range from -150°C to -20°C . The second section of testing covered a temperature region of -50°C to $+50^{\circ}\text{C}$, and the third region of testing covered a temperature region of 0°C to $+90^{\circ}\text{C}$. The resulting data were shifted to produce the frequency dependent master curve. The relaxation modulus was then calculated using the method of Ninomiya and Ferry.¹ Typical results are presented in Figures 1 and 2.

RESULTS AND DISCUSSION

Earlier work by the authors suggests that there is extensive crosslinking resulting from atomic oxygen/UV exposure, and a change in crystallinity.⁴ To understand the effect of atomic oxygen & UV radiation on the mechanical properties of these thin film materials, the control, exposed and annealed specimens will be compared. Viscoelastic measurements provide the opportunity to relate the mechanical performance of these films to their chemical structure. In particular, we are

interested in understanding the effect of changes due to the presence of atomic oxygen in the presence of UV radiation and differentiate these changes from those related to changes in crystallinity. This analysis is complicated by the fact that the crystallinity of the film was measurably reduced during exposure on the LDEF experiment.⁷ The question arises as to the definition of the sequence of events leading to changes in the crystalline structure. Wide angle and small angle x-ray analysis is underway to probe observed changes in the crystallites' structure. Earlier work suggests that the crystalline regions were crosslinked in-situ.⁷ This is evidenced by the fact that the crystalline melt temperature and the percent crystallinity for the exposed specimen were unaltered after repeated heating, suggesting a permanent morphology. If the crystalline and amorphous regions were crosslinked in-situ, one would expect the fundamental molecular relaxations to be only slightly altered. Our earlier efforts suggest that only a portion of the chains are crosslinked.⁷ At this density of crosslinking there is not enough restriction in molecular mobility to alter the fundamental relaxations in these polymers. Changes in the fundamental relaxations can be quantified by noting changes in the Arrhenius behavior of the viscoelastic shift factors. Typically, there are two quantities of importance used to analyze viscoelastic shift factors; the activation energy associated with a particular relaxation and the temperature range over which the relaxation occurs. Changes in the relaxation process will translate to a change in the activation energy for a particular relaxation (an increase in the activation energy being associated with a decrease in molecular mobility) or a change in the temperature at which the relaxation is observed. For the materials studied here, both changes are monitored.

For a molecular relaxation, the Gibbs' free energy associated with the relaxation process is classically represented by

$$\Delta G = \Delta H - T\Delta S \quad (1)$$

The rate constant associated with this relaxation process can be expressed in terms of the Gibbs free energy.

$$k = e^{-\Delta G/RT} = e^{-\Delta H/RT} e^{\Delta S/R} \quad (2)$$

The entropic term, $e^{\Delta S/R}$ is associated with the frequency at which the relaxation process takes place while the enthalpic term, $e^{-\Delta H/RT}$ is associated with the energy barrier for the process. The rate constant is inversely proportional to time; therefore, the ratio of the inverse of the rate

constant at temperature T, to the inverse of the rate constant at temperature T₀, a reference temperature, can be defined as the viscoelastic shift factor if the rate constant is a measure of the relaxation time scale. This is expressed in the equation below.

$$\frac{1/k}{1/k_0} = Ae^{\frac{\Delta H}{R} \left(\frac{1}{T} - \frac{1}{T_0} \right)} = a_T \quad (3)$$

where A is a constant. This suggests that a plot of the natural logarithm of the viscoelastic shift factor against the quantity [1/T - 1/T₀] will yield a linear expression with a slope of ΔH_a/R, the apparent activation enthalpy divided by the gas constant. For processes at constant pressure and volume, ΔH_a is equivalent to E_a, the activation energy.

Arrhenius plots derived from the construction of master curves are presented in Figures 3 to 8 for the 6 systems tested (control, annealed and exposed specimens in the machine and transverse directions). In each, the linear regions and the corresponding least squares fit used to calculate the slope (the apparent activation energy) are presented. The temperatures at which the relaxation processes change are denoted by a change in the apparent activation enthalpy. These temperatures and the corresponding activation enthalpies are summarized in the tables below.

Table 1†						
Summary of Transition Temperatures for Control, Exposed and Annealed Specimens						
<i>Annealed MD</i>	<i>Annealed TD</i>	<i>Control MD</i>	<i>Control TD</i>	<i>Exposed MD</i>	<i>Exposed TD</i>	<i>Relaxation Process</i>
61°C	66°C					α ₁
		26°C	30°C	31°C	41°C	α ₂
	-34°C		-34°C	-24°C	-29°C	β ₁
-63°C		-54°C		-68°C		β ₂

† In polyethylene, two major relaxations are recognized, the α relaxation located near 50°C and the β relaxation located near -50°C. In this summary there are clearly two "groups" of transition temperatures associated with each relaxation. For clarity in discussions, they have been designated α₁, α₂, β₁ and β₂.

Table 2
 ΔH_a (kcal/mole) for Control, Annealed and Exposed Specimen
Machine and Transverse Directions

<i>Temperature Region</i>	<i>Annealed MD</i>	<i>Annealed TD</i>	<i>Control MD</i>	<i>Control[†] TD</i>	<i>Exposed MD</i>	<i>Exposed TD</i>
<i>Above α relaxation</i>	108.9	135.7	74.9	76.7	80.0	88.8
<i>Between β and α relaxation</i>	60.3	59.6	56.5	60.6	59.2	64.4
<i>Below β relaxation</i>	21.4	29.2	17.2	-	30.0	35.9

[†] Below the β relaxation, a clearly definable linear region is not observed.

From the information provided in Tables 1 and 2, it is easy to conclude that the changes that took place aboard LDEF are not consistent with changes resulting from crystalline morphology changes. Changes in crystalline structure due to annealing and melting, as would result from thermal cycling, would lead to an increase in the activation enthalpy above the α relaxation but more importantly would result in a higher α relaxation temperature. This is not observed in the exposed specimens. The annealed specimens have an α relaxation near 60°C, a 30°C increase over that recorded for the control specimens. The exposed specimens, while showing a slight increase of 5°C to 10°C, do not demonstrate the dramatic increase associated with the annealed specimen. This would suggest that in the exposed specimens there is a slight increase in the crystalline packing (as occurs in annealed specimens) but not a significant change. This fact is further evidenced by noting the activation energies associated with the α processes. For the annealed specimens, the activation enthalpy is ~110 kcal/mole while for the control specimen the activation energy is ~75 kcal/mole. This increase is due to an increase in packing in the crystalline regions thereby increasing the barrier to molecular motion. The exposed materials show a slight ~10 kcal/mole increase in the apparent activation energy. It is therefore, easy to conclude that any observed changes in the mechanical properties of these materials is not solely due to the observed changes in crystallinity since the fundamental relaxations have not been altered to a great extent.

Earlier analysis of the exposed materials illustrated the presence of crosslinks induced by atomic oxygen/UV radiation.⁷ With this information in mind, one can conclude that the crosslinks were introduced into the polymer at an early stage of exposure before a significant amount of melting occurred. The relatively small change in the activation energies and the transition temperatures suggest that the original relaxations have somehow been preserved. In-situ crosslinking would achieve this result. This conclusion is further supported by the fact that repeated heating and cooling of the exposed material always reproduces the same extent of crystallization and the same melting temperature. This can only occur if the local structure preceding crystallization (and melting) is fixed under all conditions. In-situ crosslinking would produce this effect.

The storage and loss modulus master curves resulting from application of time/temperature superposition are presented in Figures 9 to 12. Three relaxations are visible; a relaxation centered at 10^{10} radians/second (α relaxation) with a second relaxation appearing as a shoulder centered at 1 radian/second, and a third relaxation centered at 10^{30} radians/second (β relaxation). In general, the exposed specimen shows a decrease in the E' master curve at all frequencies. There is a corresponding decrease in the E'' master curve with an additional shift to lower frequencies for the β relaxation. Although the shift is observed for the annealed specimens, there is not an observed decrease in the E' and E'' master curves. A shift to lower frequencies is equivalent to a shift to higher temperatures suggesting an increase in the energy needed to activate the β process. It has been proposed that the β transition is associated with the glass-rubber transition for the constrained amorphous chain components.^{8,9} If the proposed in-situ crosslinking mechanism does occur, one would expect to see an increase in the constraint of the amorphous segments of the polymer chain. The shift in the E'' master curve β relaxation supports this hypothesis.

Using the master curves, the relaxation modulus for each of the specimens was calculated and is compared in Figures 13 and 14. In general, for the range of times (frequencies) measured, there is an observed decrease in the modulus on exposure to LEO. However, this decrease only applies to the transient response. The long time response for all the systems measured is equivalent, the limiting modulus is the same, which suggests for the times considered, that the equilibrium mechanical behavior of these systems is unaltered by the chemical changes that take place in the polymer. Once the polymer is protected from direct exposure, the chemical changes that take place from diffusing atomic oxygen do not adversely alter the time dependent modulus.

The relaxation modulus, $E(t)$, is one measure of the mechanical or engineering performance of this material. Noting the effects of in-situ crosslinking and smaller effects due to changes in crystallinity, the engineering performance of this material is only slightly altered after exposure to

non-ram impact, atomic oxygen and UV radiation. This result does not however, speak to changes in fracture toughness, fatigue resistance, yield and failure. It only speaks to the primary engineering design property of linear viscoelastic response and modulus.

CONCLUSIONS

For the polyethylene specimen tested, it is clear that erosion typically observed in materials directly exposed to atomic oxygen has been avoided. As a result, an opportunity to study the effects of atomic oxygen with minimum UV exposure is presented. Results of this work and earlier efforts⁵ indicate a crosslinking mechanism which occurred simultaneous to thermal cycling. The result is an in-situ crosslinking that makes permanent the crystalline morphology and has little effect on the molecular relaxations associated with the amorphous chains. The exposed specimens demonstrate relaxation behavior that is similar to that of the control specimens with a measurable but small increase in the energy barrier to molecular motion for the amorphous regions. This slight decrease in molecular mobility translates to a decrease in the relaxation modulus. The long term, equilibrium relaxation moduli seem to be equivalent for the control, annealed and exposed specimen although more work is needed to clearly identify the equilibrium behavior. The observed changes in the mechanical properties (linear viscoelastic) are due to the effect of atomic oxygen and the resulting crosslinking and not do to changes in crystalline morphology.

ACKNOWLEDGEMENTS

The authors would like to thank NASA for their support in the form of research funding. In addition we would like to thank Rheometrics Inc. for their continued support.

REFERENCES

1. Ferry, J.D., "Viscoelastic Properties of Polymers", John Wiley and Sons, New York, 1980
2. Allen, D.H., in "The Long Duration Exposure Facility (LDEF). Mission 1 Experiments", Eds. Clark, L.G., Kinard, W.H., Carter, D.L., and Jones, J.L.; NASA SP-473, 1984, p.49
3. S.L. Koontz, Proceedings of the NASA/SDIO Space Environmental Effects on Materials Workshop, NASA Conference Publication 3035, Part 1, 241 (1988)
4. Letton, A., Rock, N.I., Williams, K.D., Strganac, T.W., and Farrow, D.A., "Characterization of Polymer Films Retrieved From LDEF" in First LDEF Post-Retrieval Symposium Proceedings, NASA CP-3134, p. 705, 1991

5. Strganac, T.W., Farrow, D.A., Letton, A., Williams, K.D., and Rock, N.I., "Analysis and Simulation of Polymers Exposed to Low Earth (LEO) Environments", in 30th Aerospace Sciences Meeting and Exhibit Proceedings, AIAA 92-0849, 1992
6. LDEF Spaceflight Environmental Effects Newsletter, vol.2, no. 3, June 15,1991
7. Rock, N.; Master's Thesis, Texas A & M University, College Station, Texas, December, 1992
8. Boyd, R.H.; Polymer, Vol. 26, March, pp. 323-347; 1985
9. Boyd, R.H.; Polymer, Vol. 26, August, pp. 1123-1133; 1985

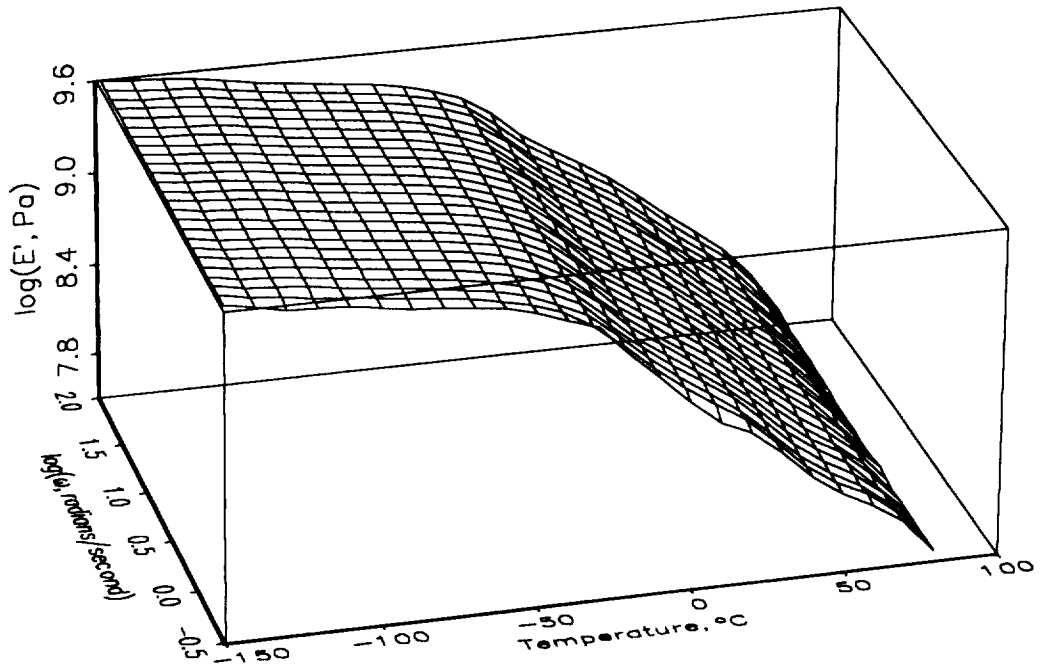


Figure 1, Typical storage modulus data. Presented is the data for the annealed specimen in the machine direction.

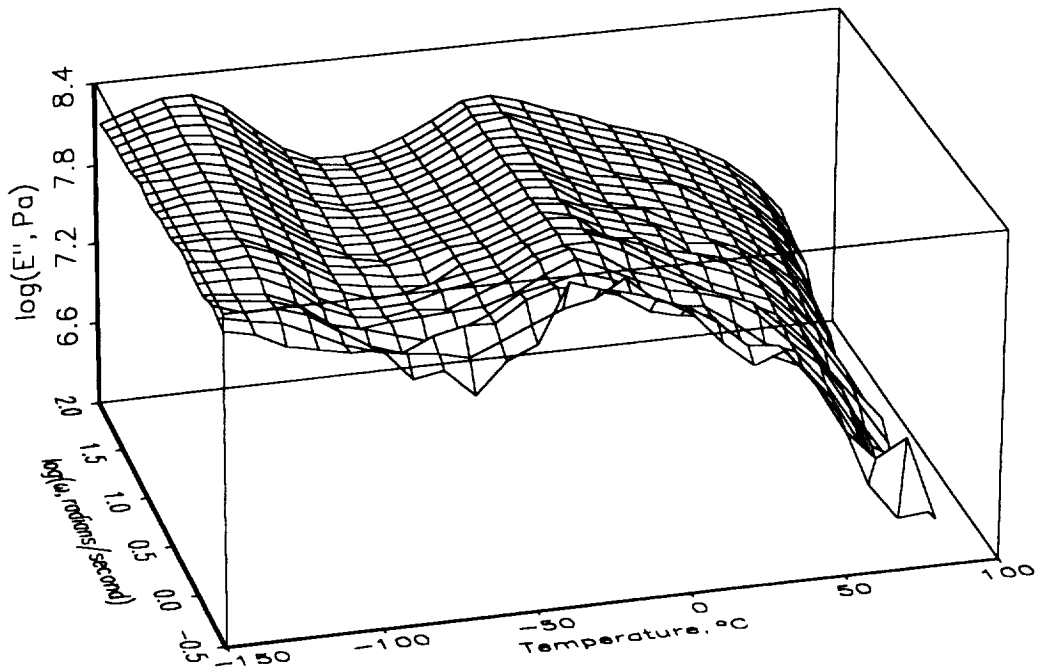


Figure 2, Typical loss modulus data for an annealed, machine direction specimen.

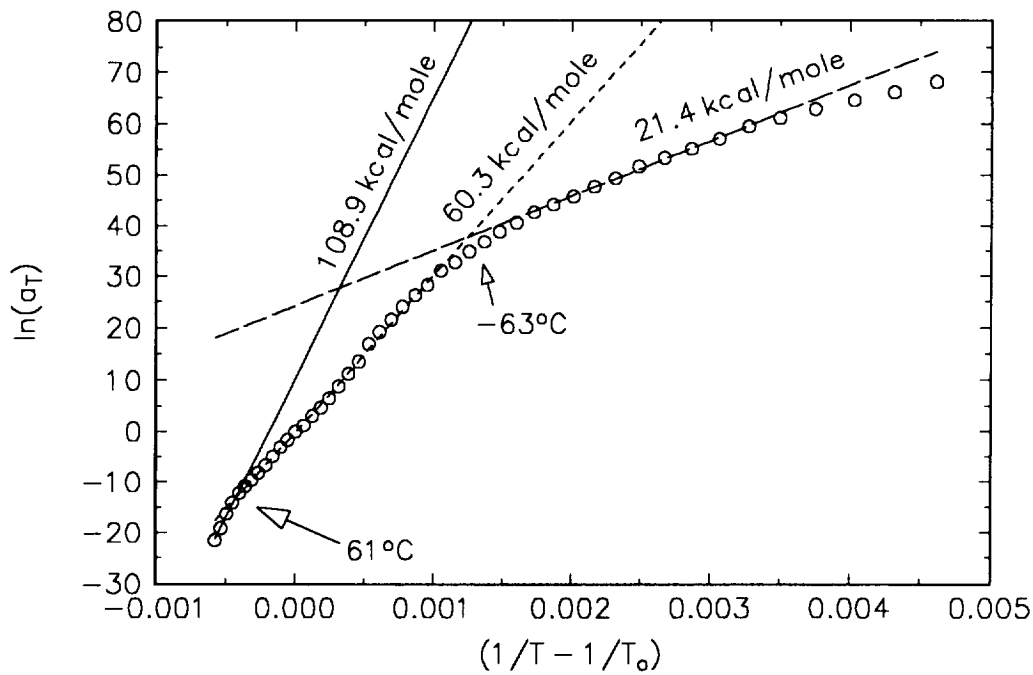


Figure 3, Arrhenius plot of viscoelastic shift factors for annealed specimen in the machine direction. Numbers by each line indicate the calculated activation energy for each relaxation while the line represents the least squares fit used to determine E_a . The arrows indicate the observed transitions and the corresponding temperatures.

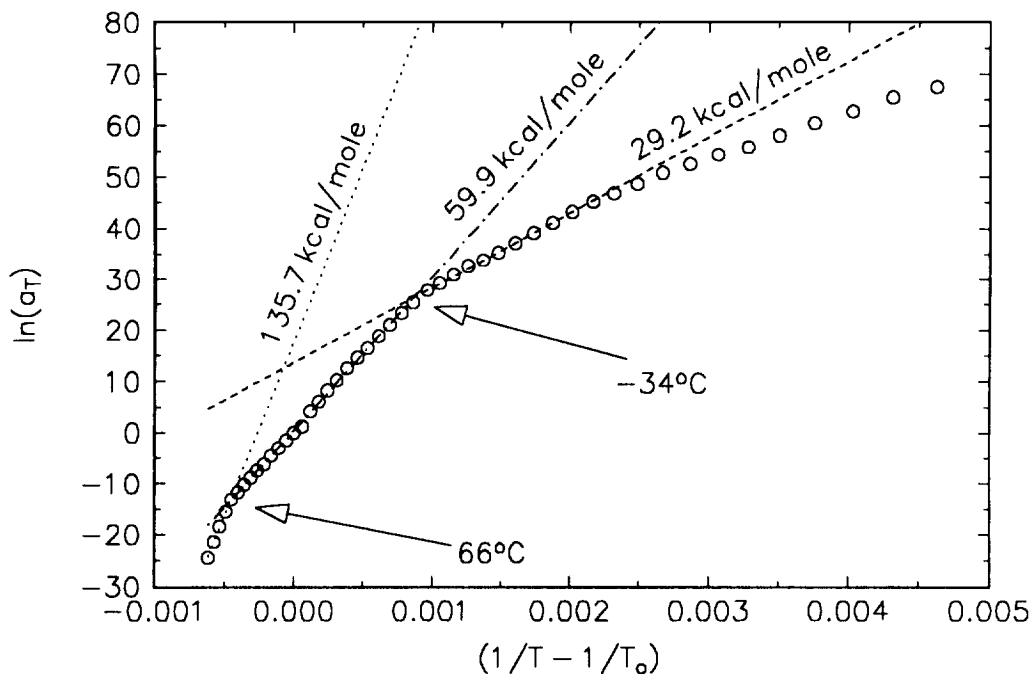


Figure 4, Arrhenius plot of viscoelastic shift factors for annealed specimen in the transverse direction. Numbers by each line indicate the calculated activation energy for each relaxation while the line represents the least squares fit used to determine E_a . The arrows indicate the observed transitions and the corresponding temperatures.

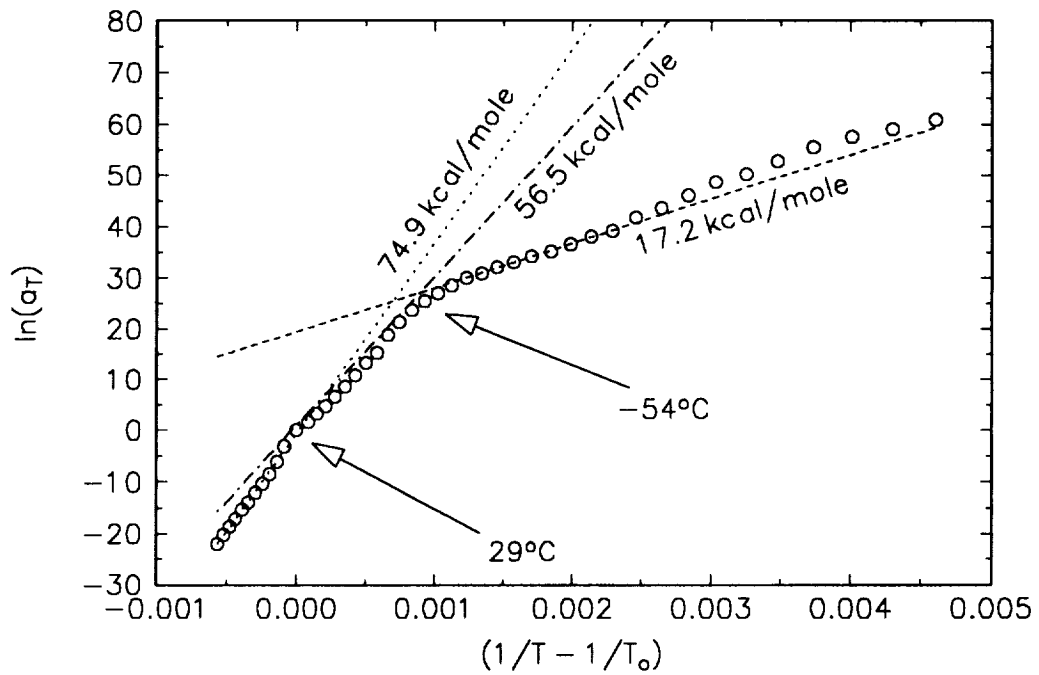


Figure 5, Arrhenius plot of viscoelastic shift factors for the control specimen in the machine direction. Numbers by each line indicate the calculated activation energy for each relaxation while the line represents the least squares fit used to determine E_a . The arrows indicate the observed transitions and the corresponding temperatures.

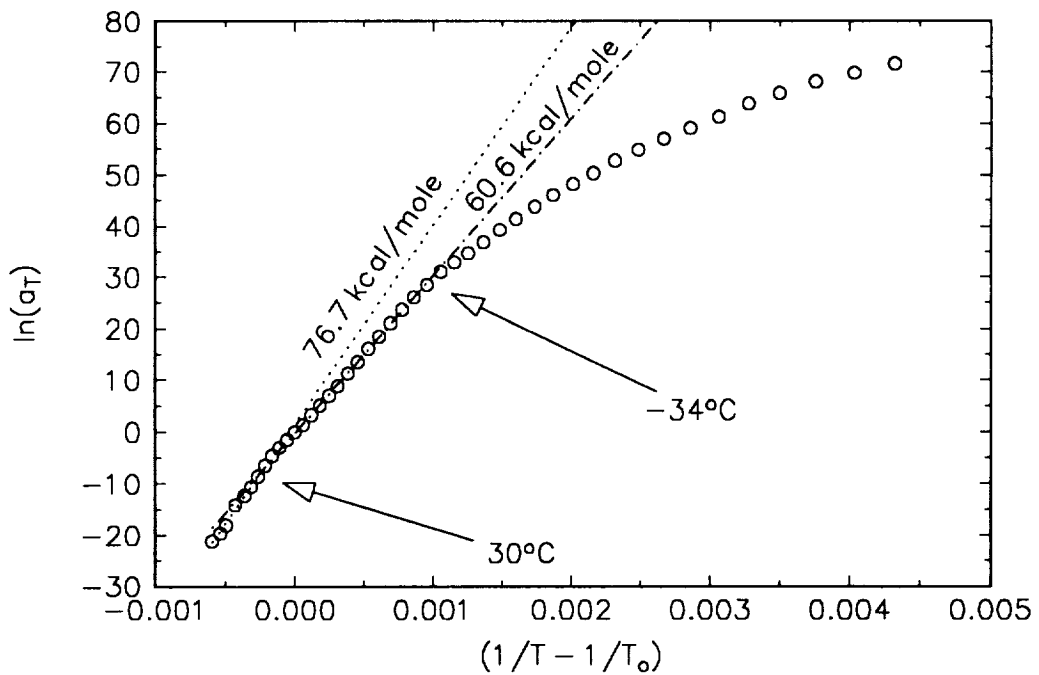


Figure 6, Arrhenius plot of viscoelastic shift factors for the control specimen in the transverse direction. Numbers by each line indicate the calculated activation energy for each relaxation while the line represents the least squares fit used to determine E_a . The arrows indicate the observed transitions and the corresponding temperatures.

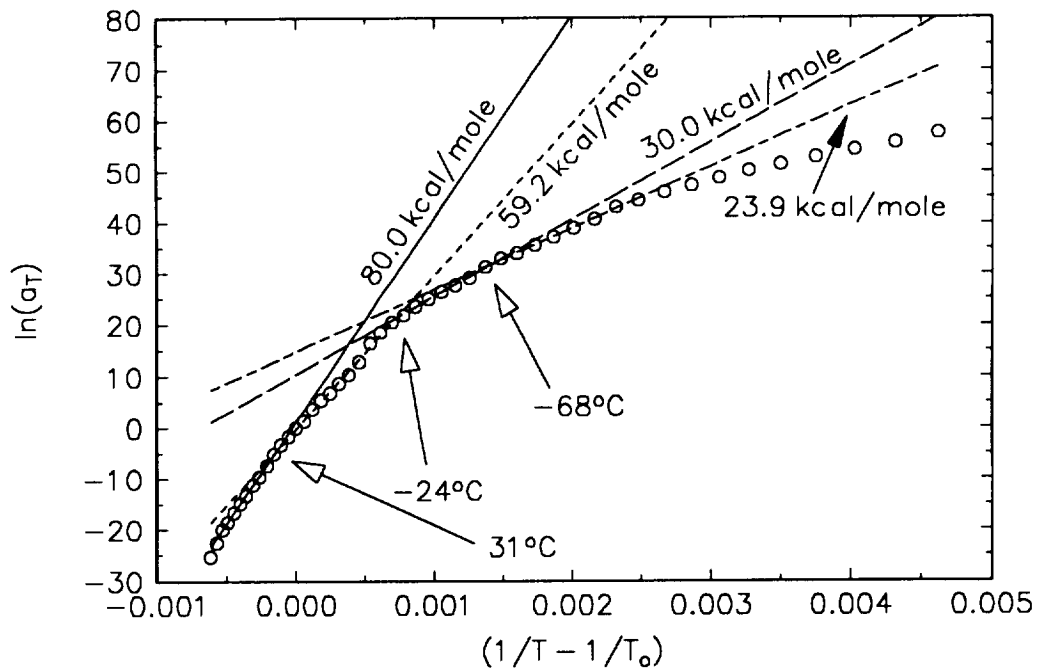


Figure 7, Arrhenius plot of the viscoelastic shift factors for the exposed specimen in the machine direction. Numbers by each line indicate the calculated activation energy for each relaxation while the line represents the least squares fit used to determine E_a . The arrows indicate the observed transitions and the corresponding temperatures.

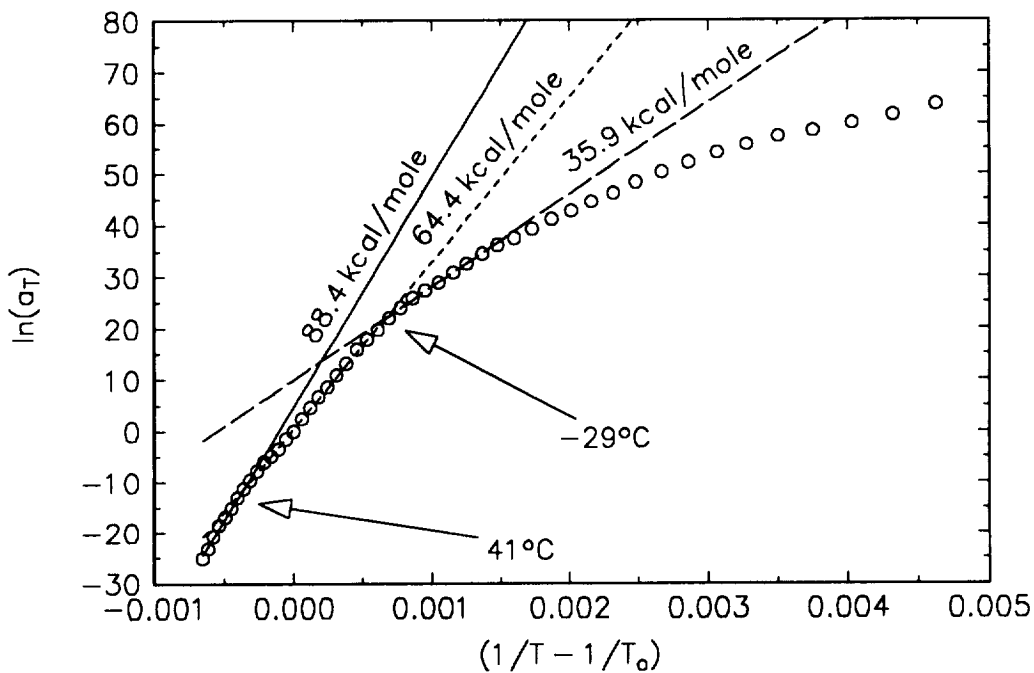


Figure 8, Arrhenius plot of the viscoelastic shift factors for the exposed specimen in the transverse direction. Numbers by each line indicate the calculated activation energy for each relaxation while the line represents the least squares fit used to determine E_a . The arrows indicate the observed transitions and the corresponding temperatures.

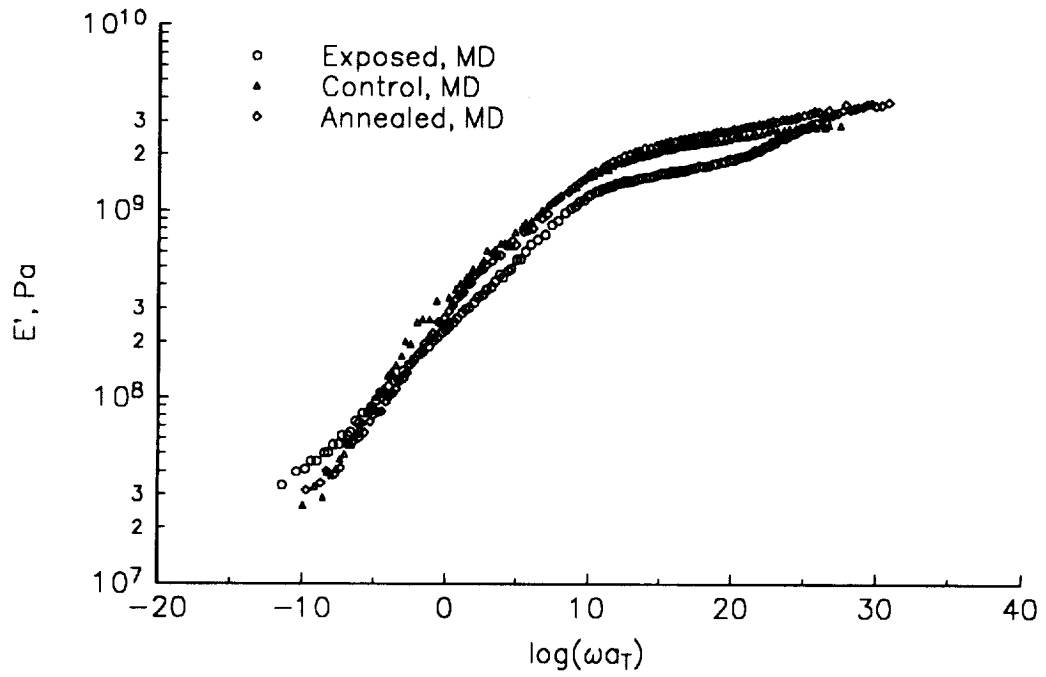


Figure 9, E' master curve for specimen in the machine direction. Every third point is plotted for clarity.

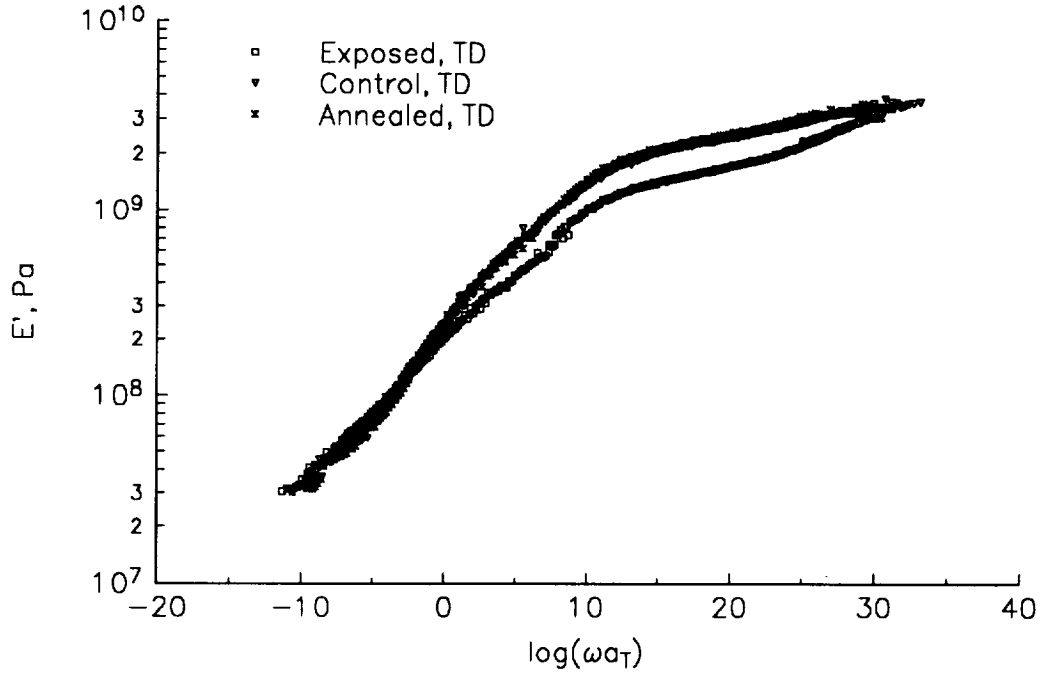


Figure 10, E' master curve for specimen in the transverse direction. Every third point is plotted for clarity.

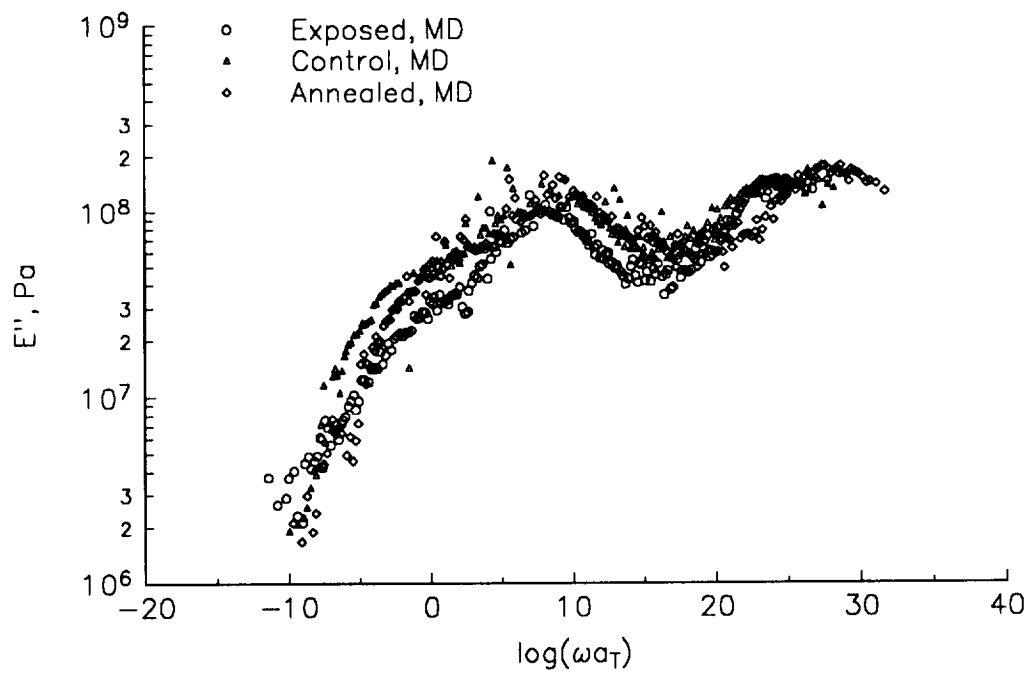


Figure 11, E'' master curve for specimen in the machine direction. Every third point is plotted for clarity.

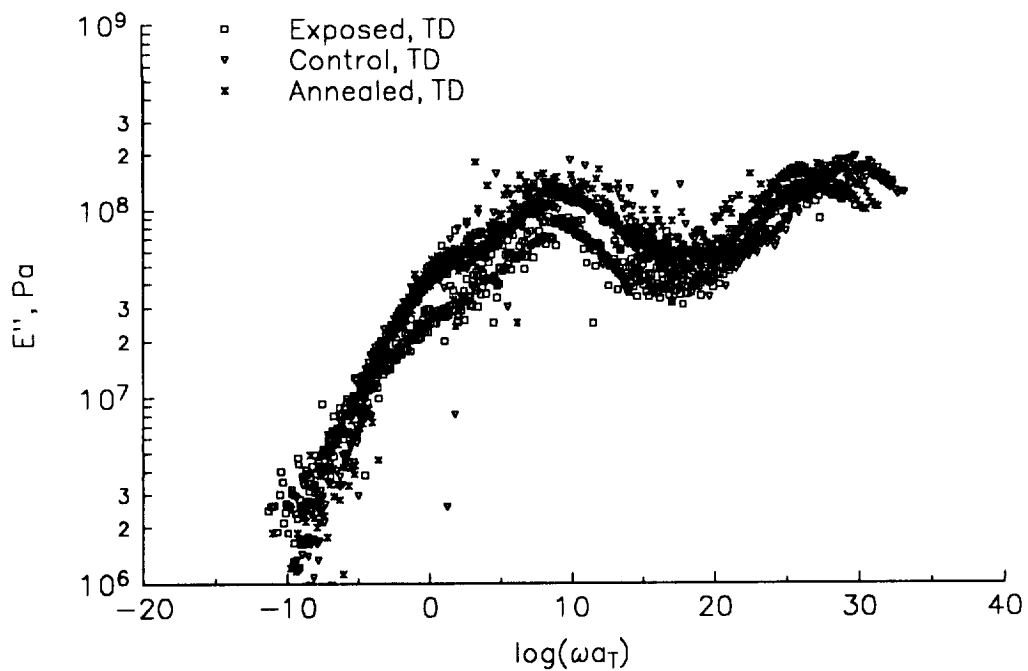


Figure 12, E'' master curve for specimen in the transverse direction. All points are included.

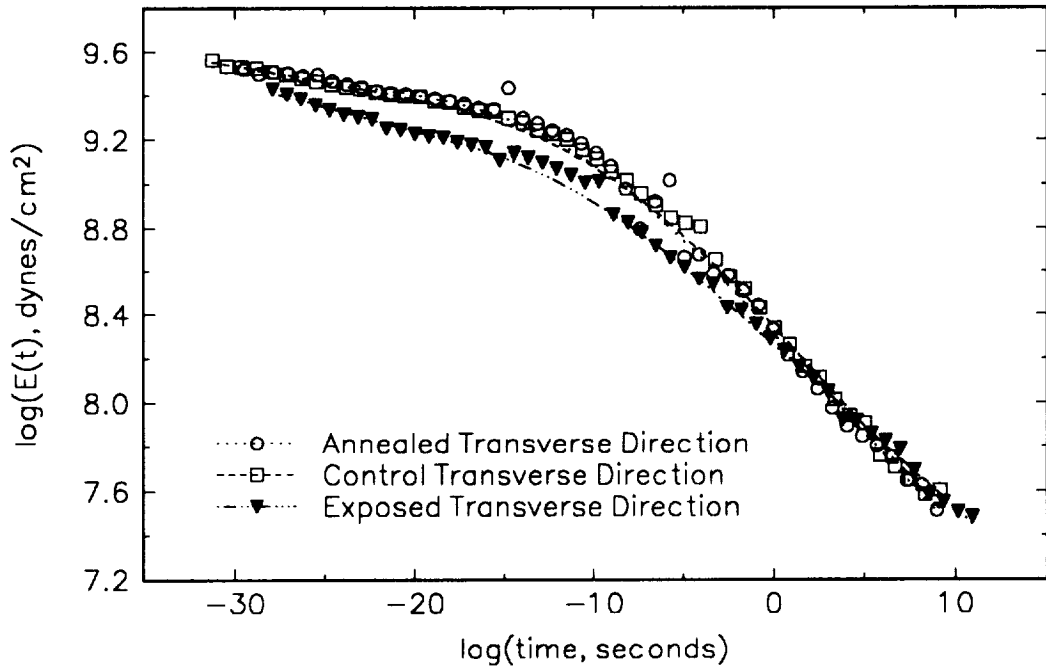


Figure 13, Relaxation modulus calculated for specimens with a transverse orientation.

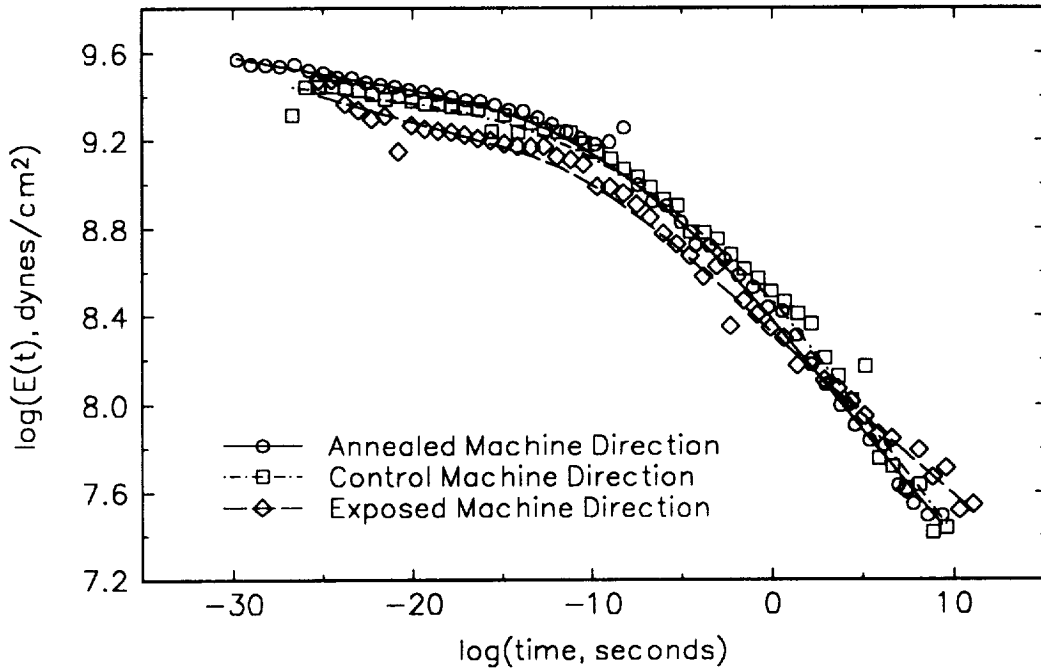


Figure 14, Relaxation modulus calculated for specimens with a machine direction orientation.